



5TH GENERATION SEISMIC HAZARD MODEL FOR NORTH-WESTERN CANADA

Trevor I. ALLEN

Seismologist, Geological Survey of Canada, Sidney, Canada
tallen@nrcan.gc.ca

John ADAMS

Seismologist, Geological Survey of Canada, Ottawa, Canada
jadams@nrcan.gc.ca

Stephen HALCHUK

Seismologist, Geological Survey of Canada, Ottawa, Canada
shalchuk@nrcan.gc.ca

Garry C. ROGERS

Seismologist, Geological Survey of Canada, Sidney, Canada
grogers@nrcan.gc.ca

ABSTRACT: The Geological Survey of Canada has recently completed national seismic hazard models prepared to underpin the seismic provisions for the 2015 National Building Code of Canada. This contribution summarises the reassessment and revision of earthquake sources in the western Canadian Arctic, northern British Columbia and adjacent Alaska. Area sources are defined through a multi-tiered approach in a GIS framework. The key thematic layers used to guide the area source boundaries are: historical earthquake epicentres; tectonic elements; gravity and magnetic anomalies; and multi-resolution topography and bathymetry.

For the first time, hazard from crustal faults in Yukon, and adjacent Alaska is calculated based on GPS- and paleoseismic-based slip rates. Maximum magnitude for each fault source is determined from published magnitude-area scaling relations. Hazard along the Queen Charlotte and Fairweather faults is also now predominantly based on crustal deformation rates, with minor contributions to off-fault hazard assessed from historical seismicity. In recognition of the M_w 7.8 2012 Haida Gwaii thrust earthquake, we partition the slip between the strike-slip Queen Charlotte fault and the shallow-dipping Haida Gwaii thrust that is modelled as a subduction source.

A regional tectonic model for northwestern Canada, supported by GPS deformation rates and earthquake focal mechanisms (Leonard et al., JGR, 2007), suggests that observed northerly motion from southern Yukon Territory continues to the Beaufort Sea margin. The inferred convergence in the Mackenzie Delta region could manifest itself through infrequent large earthquakes with very few small events. Based on this hypothesis, a new Beaufort-Mackenzie Convergence zone allows for the possibility of seismogenic thrusting (up to M_w 7.8) beneath the delta sediments.

1. Introduction

The Geological Survey of Canada (GSC), a branch of Natural Resources Canada, is responsible for providing seismic hazard information to safeguard Canadian citizens and to minimise the negative impacts of earthquakes. The proposed hazard models (Adams *et al.*, 2015) are intended to form the basis

for the seismic provisions in the 2015 edition of the National Building Code of Canada (NBCC). This contribution outlines the rationale behind the development of hazard-model inputs for the western Canadian Arctic (approximately north of 60°N latitude), as well as the newly-implemented shallow crustal faults for the western margin (excluding Cascadia).

The seismicity of northern Canada was first described by Basham *et al.* (1977). They identified broad zones of seismicity with highly variable rates of earthquakes. In particular, Basham *et al.* (1977) identified high rates of seismicity in the Yukon – Mackenzie Valley region, which are well-correlated with major crustal deformation (e.g. Hyndman *et al.*, 2005b; Leonard *et al.*, 2007). The northern continental passive margin was also identified as a region of higher than average seismicity, particularly in the Beaufort Sea and Queen Elizabeth Shelf region to the east. In conclusion, Basham *et al.* (1977) suggested that the seismicity of northern Canada was characterised by frequent swarm activity, diffuse bands of small-to-moderate earthquakes, and occasional large earthquakes. The physical mechanism for the occurrence of these earthquakes was thought to vary from plate boundary forces, post-glacial uplift, or through stresses induced from uncompensated sedimentary loads (Basham *et al.*, 1977).

The discussion on the hazard parameters provided herein (e.g., areal source zones, magnitude-frequency statistics, and fault models) form the basis for the inputs to the GSC's 5th Generation Seismic Hazard Model of Canada (2015SHMC) in the western Arctic region (Halchuk *et al.*, 2014).

2. Modelling Western Arctic Areal Sources

Areal source zones are used in probabilistic seismic hazard analyses to define regions that are approximated to produce earthquakes randomly and with equal likelihood anywhere. Area sources are often used to account for “background” seismicity, or for earthquakes that are not associated with any specific fault (Baker, 2008). We define area sources for the western Arctic through a multi-tiered approach in a Geographic Information Systems (GIS) framework (e.g., Brown and Gibson, 2004). Thematic features (e.g. points, lines, or polygons), together with their attributes, and raster data, are integrated within an ESRI ArcGIS™ geodatabase. The key thematic layers guiding the classification of area sources are:

- Historical earthquake epicentres (Halchuk *et al.*, 2015)
- Tectonic Map of Canada (Stockwell, 1968)
- Gravity Anomaly Map of Canada and Alaska (Miles *et al.*, 2000a; Saltus *et al.*, 2008)
- Magnetic Anomaly Map of Canada and Alaska (Miles *et al.*, 2000b; Bankey *et al.*, 2002)
- Multi-resolution topography and bathymetry (e.g., GEBCO, 2008)

Source zones were digitised as ESRI ArcGIS™ shapefiles, allowing each polygon to have its spatial attributes joined with additional information, such as zone name, area, earthquake magnitude-frequency distribution (MFD) and maximum magnitude earthquake, M_{max} . The zone boundaries were chiefly based on the historical earthquake catalogue. They were subsequently refined using additional geological and geophysical information (Fig. 1). The rationale for this refinement is to allow for areas of similar geological and geophysical characteristics to host similar rates of temporally varying earthquakes that may not be captured in the historic record. The migration of earthquake activity in space is more commonly observed in Stable Continental Regions (SCRs) that are characterised by long return periods on a given fault (e.g., Clark *et al.*, 2012; Liu and Wang, 2012).

The area sources were subsequently used to calculate Gutenberg-Richter magnitude-frequency statistics (Gutenberg and Richter, 1944; Weichert, 1980) from the historical earthquake catalogue (Halchuk *et al.*, 2015) using the maximum likelihood technique (Aki, 1965).

The areal source zones of the western Arctic model are coupled with recurrence estimates from active faults in Alaska and Yukon Territory using long-term slip rates from GPS and information from paleoseismic studies. It is assumed that onshore earthquakes in the western Arctic catalogue represent the hazard from distributed seismicity and are not related to slip on the modelled fault sources. This assumption potentially represents an overestimation of earthquake rates in zones through which the fault sources pass since some of the historical seismicity may be associated with the modelled faults.

However, this effect is minimised by the choice of a relatively high minimum magnitude, M_{min} , for the fault sources (Table 1). In most cases, ruptures along these fault sources have not occurred in the historical era. Thus, future earthquakes along these faults are considered characteristic in nature (Youngs and Coppersmith, 1985), that is, their rates are not directly related to the rates of background earthquakes.

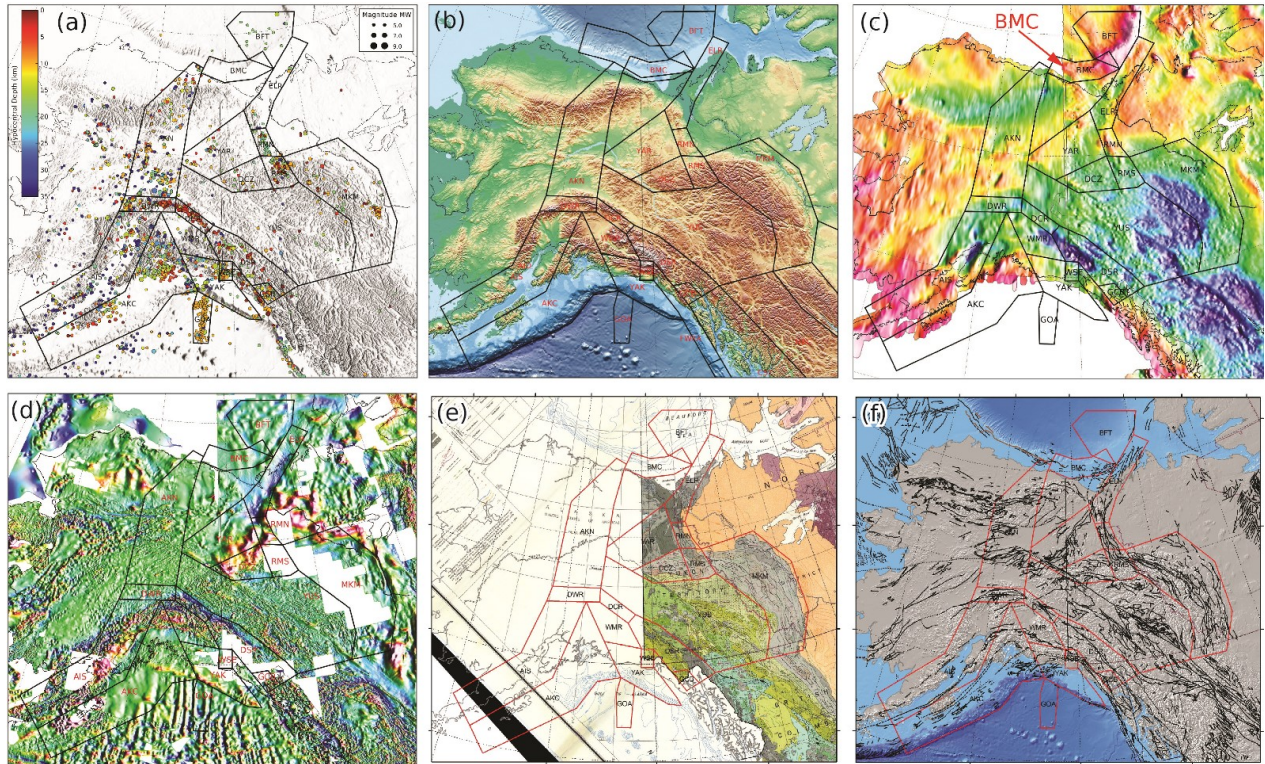


Figure 1 – Areal source zones for the western Arctic, based on: a) historical seismicity; b) topography and bathymetry; c) gravity; d) magnetics; e) tectonic elements, and; f) crustal structure (faults).

3. Modelling Fault Sources

For the first time in the western Arctic, the 2015SHMC incorporates hazard contributions from crustal fault sources. The hazard parameters from these crustal fault sources are characterised by long-term slip rates determined from Global Positioning System (GPS) measurements and paleoseismic observations in Canada and across the international border in Alaska. Using published slip rates with an upper and lower bound (Table 1), the average seismic moment rates \dot{M}_0 are estimated for offshore and onshore crustal faults (e.g. Youngs and Coppersmith, 1985) following:

$$\dot{M}_0 = \mu AS \quad (1)$$

where \dot{M}_0 is measured in N-m/yr, μ is the shear modulus (or crustal rigidity) in Pa and A is the total fault area. Bilek and Lay (1999) have shown that when a constant stress drop (e.g. Brune, 1970) is assumed, the frictional behaviour of faults in subduction zones indicate increasing rigidity as depth increases. Rigidity is commonly taken to be $\mu = 30$ GPa for crustal earthquakes (e.g. Brune, 1970). However, since offshore sediments are often less-consolidated, it could be assumed that the shear modulus of these sediments would be less than assumed for crustal earthquakes. Consequently, for offshore fault sources, we assume $\mu = 20$ GPa.

With estimates of the seismic moment rate based on the inferred slip rate and fault area, we can invert for the number of earthquakes per year with magnitude greater than or equal to zero, N_0 following (e.g., Hyndman and Weichert, 1983; GEM Foundation, 2012):

$$N_0 = 10^{A_0} \quad (2)$$

and:

$$A_0 = \log \left\{ \frac{M_0^{(c-b)}}{10^{(c-b)M_{max}} - 10^{(c-b)M_{min}}} \right\} - d - \log b \quad (3)$$

where M_{min} is the lowest magnitude for the magnitude-frequency distribution and the coefficients c and d relate magnitude m to seismic moment (e.g. Hanks and Kanamori, 1979):

$$\log M_0 = cm + d \quad (4)$$

In the present study, we assume m is equivalent to moment magnitude M_W . Finally, a bounded Gutenberg-Richter MFD is estimated following:

$$N(m) = N_0 e^{-\beta m} [1 - e^{-\beta(M_{max}-m)}] \quad (5)$$

where N is the cumulative number of earthquakes greater than magnitude m and β is a constant that describes the relative number of small-to-large earthquakes, where $\beta = b \ln(10)$ and b is the G-R b -value. The available seismic moment rate is distributed across earthquakes from M_{min} through to M_{max} using two b -values with a weight of 0.5 each in the hazard calculation: the first having a b -value of 0.8, and the second being near-zero ($b = 0.0001$) to approximate a characteristic earthquake distribution (Youngs and Coppersmith, 1985). Herein, the latter form of distributions are referred to as pseudo-characteristic MFDs. Due to limitations in GSC's hazard computation software, the functional form of the characteristic magnitude-frequency distribution could not be incorporated directly into the model.

Table 1 – Slip rates (in mm/yr) used for fault magnitude-frequency distributions.

Fault Name	Slip Rate Best	Slip Rate Min	Slip Rate Max	M_{min}	M_{max}^*	Reference
Eastern Denali	2	1	4	6.5	7.9	Fletcher and Freymueller (2003); Cassidy/Mazzotti, pers comm (2013)
Central Denali - Totschunda	6	5	7	6.5	7.8	Matmon <i>et al.</i> (2006)
Western-Central Denali	8	6	10	6.5	7.9	Matmon <i>et al.</i> (2006)
Duke River	3.5	1	7	6.5	7.7	Leonard <i>et al.</i> (2008)
Chatham Strait	2	1	2	6.5	7.8	Wesson <i>et al.</i> (2007)
Queen Charlotte [‡]	44 [†]	42 [†]	46 [†]	6.5	8.2	Fletcher and Freymueller (2003); Mazzotti <i>et al.</i> (2003)
Fairweather [‡]	46	44	48	6.5	8.3	Fletcher and Freymueller (2003)
Haida Gwaii Thrust	13	11	15	7.0	8.0	Mazzotti <i>et al.</i> (2003)
Winona Thrust	13	11	15	7.0	7.4	Leonard <i>et al.</i> (2012)
Beaufort Mackenzie Convergence	2	1	3	7.0	7.8	Leonard <i>et al.</i> (2007)

* M_{max} estimated for strike-slip faults based on the average of several magnitude-area scaling relationships (e.g., Wells and Coppersmith, 1994; Hanks and Bakun, 2002; Shaw, 2009; Leonard, 2010). Crustal thrust faults are based on the average of Wells and Coppersmith (1994) and Leonard (2010) magnitude-area scaling relationships. Offshore thrust faults use Strasser *et al.* (2010).

[†] Modified from Fletcher and Freymueller (2003) to account for slip partitioning onto the Haida Gwaii Thrust based on Mazzotti *et al.* (2003) slip rates.

[‡] Values in table further reduced by a factor of 0.95 to account for off-fault seismicity within broad deformation zones about the faults.

4. Offshore Fault Sources in Western Canada

4.1. Queen Charlotte and Fairweather Strike-Slip System

Regionally, the Pacific plate (PA) is moving in a north-northwestwardly direction relative to stable North America (NA). The relative plate velocity increases from 46.5 mm/a south of Moresby Island to approximately 50 mm/a off the Alaska Panhandle (DeMets and Dixon, 1999; Mazzotti *et al.*, 2003). The Queen Charlotte strike-slip fault (QCSS) accommodates most of the relative PA/NA plate motion. This fault extends from just south of Moresby Island, southern Haida Gwaii, transitioning to the Fairweather fault (FWF) where it enters continental Alaska. The central segment of the QCSS ruptured in a M_S 8.1 strike-slip earthquake in 1949 – Canada's largest instrumentally recorded earthquake (Lamontagne *et al.*, 2008). While the rupture length of the 1949 event is still uncertain (estimates are in the range 265–490 km), the best evidence suggests a bilateral rupture from the epicenter off Graham Island, with the largest displacements occurring north of the epicenter (e.g., Nishenko and Jacob, 1990).

For the 4th Generation model, a narrow areal source that encompassed the historical seismicity along the combined QCSS-FWF system was used to model the MFD for the fault source up to the assumed M_{max} of 8.5 (Adams and Halchuk, 2003). The calculated hazard for the 5th Generation model uses simple line sources to approximate the QCSS and FWF, but separates the two fault segments. The M_{max} of each fault segment is based on their respective fault areas (see Table 1). These line sources represent vertical transform faults extending from the ocean bottom to 20 km depth. The slip rates used to determine the MFDs were adjusted from values in Table 1 to allow 5% of the measured deformation to be caused through off-fault activity. The Gutenberg-Richter and pseudo-characteristic MFDs for the fault sources were determined using these adjusted slip rates and the parameters in Table 1.

The QCSS and FWF sources are enclosed by narrow areal sources in a similar manner to the 4th Generation hazard model; the Queen Charlotte Fault Area (QCFA) and Fairweather Fault Area (FWFA) sources, respectively (Fig. 2). These areal sources are designed to capture off-fault seismicity within the deformation zone. Gutenberg-Richter MFDs for the areal sources were calculated based on the historical catalogue and a M_{max} of 6.7. To ensure minimal double-counting of seismicity between the fault and area sources, the resulting MFD for QCFA was used to estimate an approximate slip rate due to off-fault seismicity by inverting Equations 1 through 5. Based on the historical seismicity within the QCFA source, the contribution to the total slip-rate from the off-fault activity was estimated to be 5.9% of the total long-term slip rate; approximately equivalent to the 5% reduction applied in estimating the QCSS MFD.

4.2. Haida Gwaii Thrust

The 28 October 2012 M_W 7.8 earthquake occurred on a shallow-dipping thrust fault that partitions compressional strain from the steeply-dipping strike-slip QCSS (James *et al.*, 2013). The existence of the Haida Gwaii thrust had previously been proposed and arguments for its existence are summarized in Hyndman and Hamilton (1993) and Hyndman (2015). The hypothesis of convergence along this thrust is supported by GPS crustal velocity vectors (Mazzotti *et al.*, 2003). Due to the generation of the accretionary sedimentary prism (the Queen Charlotte Terrace), the fault system is considered to be subduction in nature, with the Pacific plate underthrusting the terrace and Haida Gwaii islands beneath the QCSS (Hyndman and Hamilton, 1993).

The modelled margin-normal component of the PA/NA motion is observed to vary from 15 to 8 mm/yr from the southern to northern extents of Haida Gwaii. At the latitude of the GPS sites in northern Moresby Island, the convergence is approximately 13 mm/yr (Mazzotti *et al.*, 2003).

The updip edge of the modelled Haida Gwaii thrust fault (HGT) was based upon the geometry of the accretionary prism, west of the QCSS. The HGT was modelled with a length of almost 360 km, from just south of Moresby Island to north of Graham Island near the southern extent of the Alaska Panhandle (Fig. 2). The HGT is modelled with an estimated dip of 25° from the sea floor (modelled at 2 km depth) to a depth of 22 km. Modelling by Wang *et al.* (2015) suggests that the down-dip extent of the HGT, near the Haida Gwaii coastline, is limited by thermal constraints landward of the QCSS fault. The area of the modelled fault is approximately a factor of two larger (mostly longer) than the modelled area from the 2012 M_W 7.8 Haida Gwaii fault source (e.g., Lay *et al.*, 2013).

The M_{max} of the HGT was based on the modelled rupture area and used the subduction interface magnitude-area equations of Strasser *et al.* (2010). The preferred M_{max} is estimated at 8.0, which is consistent with the 2012 earthquake rupturing half of the available fault area. Gutenberg-Richter and pseudo-characteristic earthquake MFDs were subsequently generated using Equations 1 through 5, assuming a minimum magnitude of M_{min} 7.0.

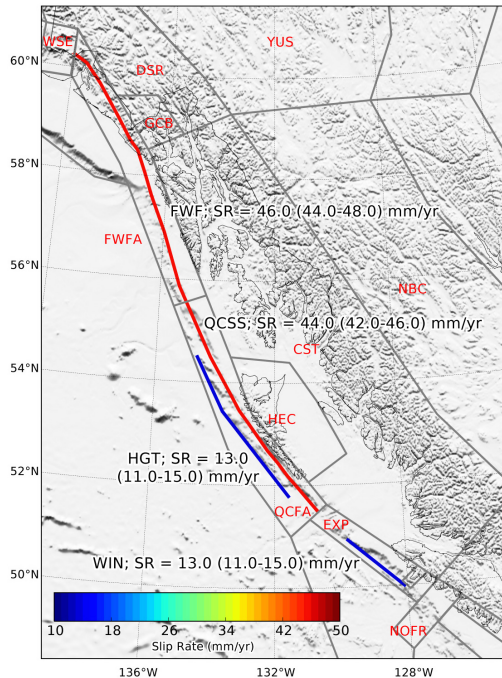


Figure 2 – Surface projection of offshore fault sources north of the Explorer plate coloured by slip rate. Published slip rates are used to estimate the seismic moment rate and develop magnitude-frequency distributions. FWF = Fairweather fault; QCSS = Queen Charlotte Strike-Slip fault; HGT = Haida Gwaii thrust fault, and; WIN = Winona thrust block. Fault sources are coloured by slip rate.

4.3. Winona Block Thrust

The Winona Block is a deep sedimentary basin along the base of the continental margin northwest of Vancouver Island (Davis and Riddihough, 1982). The basin abuts the Explorer Plate to the southeast and is bounded to the west by the Revere-Dellwood-Wilson transform fault (Braunmiller and Nábělek, 2002). The basin is comprised of deformed sediments that indicate convergence between the Winona Block and North America (Davis and Riddihough, 1982). This convergence appears to vary from near zero in the northwest to values likely consistent with the adjacent Explorer Plate in the southeast. High heat flow and the lack of any observable slab north of Vancouver Island (Yuan *et al.*, 1992; Cassidy *et al.*, 1998) suggests that convergence along the margin is young; possibly limited to 30 km in 2 Ma (Braunmiller and Nábělek, 2002).

Whilst the historic earthquake record does not indicate active subduction of the oceanic lithosphere beneath North America, the presence of an apparent accretionary prism (Davis and Hyndman, 1989), coupled with deformed sediments within the Winona Block, suggest ongoing convergence (Davis and Riddihough, 1982; Braunmiller and Nábělek, 2002). Paleoseismic evidence for the region has not yet been investigated. Given our limited understanding of the Winona system and its potential to generate large thrust earthquakes, we allow for the possibility of both large rare earthquakes along the deformation front and aseismic slip (i.e., no large earthquakes) with an equal weight of 0.5.

The top edge of the southeasterly-dipping plane was defined along the accretionary prism with a length of 155 km (Fig. 2). Near the prism, gently dipping basement at approximately 9° is inferred to be the top of the subducting oceanic crust (Yuan *et al.*, 1992). However, it is expected that the slab dip will increase landward of the trench axis. Based on expert opinion (pers. comm. E. Davis and R. Hyndman), we assume a dip of 15° and a narrow down-dip fault width of 10 km. Using the magnitude-area scaling relations of Strasser *et al.* (2010) for subduction interface environments, our preferred characteristic magnitude M_C is 7.14 ± 0.29 . The maximum possible magnitude M_{max} is thus taken as $M_C + 0.25$ (Youngs and Coppersmith, 1985).

Slip rates for the Explorer fault (S_{EXP}) and the combined Explorer-Winona source (S_{TOT}) are provided by Leonard *et al.* (2012). We assume the slip rate of the combined sources is proportional to the length of the individual sources. Assuming $S_{EXP} = 16.2$ mm/yr and $S_{TOT} = 22.5$ mm/yr for the best model, the slip between the Explorer fault and Winona block is partitioned according to:

$$S_{WIN} = \text{floor}[(S_{TOT}L_{TOT} - S_{EXP}L_{EXP})/L_{WIN}] \quad (6)$$

where S_{WIN} is the slip rate in mm/yr and L_{WIN} is the fault length for the Winona Block. Using data provided by Leonard *et al.* (2012) and Equation 6, we calculate an approximate convergence of 13 ± 2 mm/yr for the Winona thrust block. Despite the apparent south-easterly increase in slip rate towards the Explorer Plate (Davis and Riddihough, 1982), we approximate a uniform slip rate across the modelled fault source.

Magnitude frequency distributions were subsequently calculated from the seismic moment rate based on the fault area, M_{max} , S_{WIN} (see Equations 1 through 5) and additional parameters in Table 1. Both Gutenberg-Richter and pseudo-characteristic MFDs were calculated according to the methods outlined in Section 3 above. Traditional areal source zones are used to model the background seismicity about the Winona Block using MFDs from the historical catalogue (Halchuk *et al.*, 2014; 2015). The logic tree used in the 2015 SHMC for slip-derived hazard from the Winona Thrust Block is shown in Figure 3.

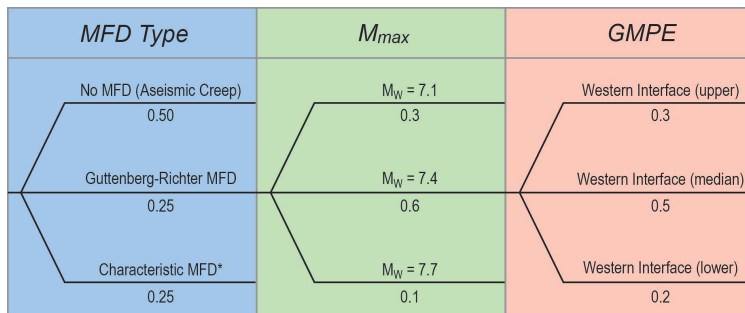


Figure 3 – Logic tree for slip-derived hazard from the Winona Thrust Block (WIN).

5. Crustal Fault Sources in Western Canada

5.1. Denali-Totschunda Fault System

The Denali-Totschunda fault system is a major strike-slip fault (Fig. 4) that accommodates deformation of interior Alaska associated with the Yakutat plate convergence (Matmon *et al.*, 2006). The 3 November 2002 M_W 7.9 Denali, Alaska earthquake resulted in a 341 km surface rupture from west to east along the Denali and Totschunda faults, with average right-lateral displacements of 4.5-5.1 m (Haeussler *et al.*, 2004). Long-term slip rates along Denali-Totschunda fault system in the western and central segments of the Denali fault (as defined herein) are generally estimated at 8-12 mm/yr, with the largest rates inferred near the intersection with the Totschunda fault (Matmon *et al.*, 2006). Further east into the Yukon Territory, slip along the Denali fault decreases to about 1 mm/yr (Kalbas *et al.*, 2008).

A simplified fault model is developed that conserves slip along Denali-Totschunda fault system. The Western-Central Denali (WCD) is a 470 km fault segment that spans from the western Denali (Matmon *et al.*, 2006) through to near the Alaska-Yukon Territory border modelled with a uniform slip rate of 8 mm/yr (Fig. 4). The 420 km-long Central Denali-Totschunda (CDT) fault segment extends the 2002 Denali rupture along the Totschunda fault and partitions slip from the central Denali fault. The CDT segment is modelled using a uniform slip rate of 6 mm/yr. Much of the CDT segment superimposes the WCD segment and results in a cumulative slip rate of 14 mm/yr in overlapping regions, consistent with Matmon *et al.* (2006). The Denali fault is modelled into Yukon using the Eastern Denali Fault (EDF) transferring to the Chatham Strait Fault (CSF) with modelled slip rates of 2 mm/yr (Fletcher and Freymueller, 2003) and 1 mm/yr (Wesson *et al.*, 2007), respectively.

Modelling the magnitude-frequency distribution along these faults assumes M_{min} of 6.5. To ensure we capture an overlapping magnitude range, $M_{max} = 6.7$ is used for the surrounding areal source zones which express a uniform hazard for the region based on diffuse historical seismicity. To prevent aftershocks from the 2002 sequence influencing the hazard estimates for the areal sources, MFDs are calculated from a temporally truncated catalogue that only includes events up to and including the 2002 M_W 7.9 Denali earthquake.

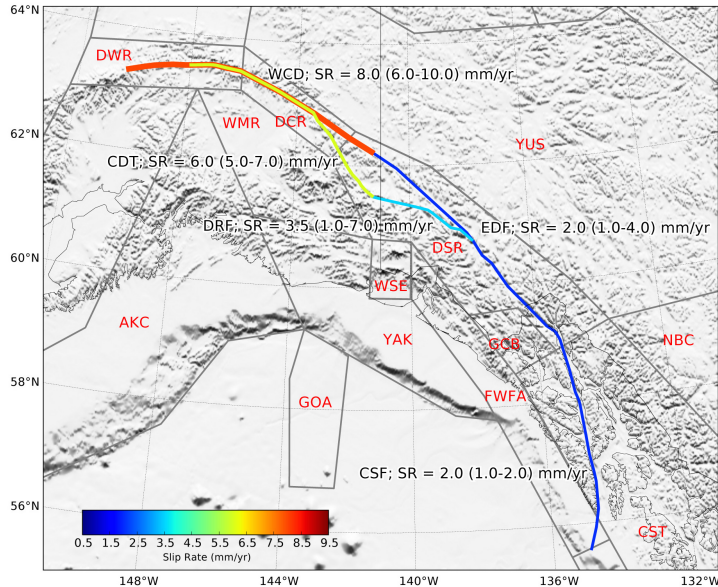


Figure 4 – Surface projection of crustal fault sources in Yukon and Alaska coloured by slip rate. Published slip rates are used to estimate the seismic moment rate and develop magnitude-frequency distributions. WCD = Western-Central Denali fault; CDT = Central Denali-Totshunda faults; EDF = Eastern Denali fault, and; DRF = Duke River fault.

5.2. Duke River Fault

The Duke River fault is a terrane-bounding structure in southwestern Yukon that deforms Miocene-to-Pliocene-aged Wrangell volcanics (Cobbett *et al.*, 2010). Originally interpreted as a post-Triassic dextral strike-slip fault that accommodated major displacements (Clague, 1979), the Duke River fault is now thought to have been reactivated with oblique reverse movement based on earthquake focal mechanisms (Power, 1988) and geological interpretations (Cobbett *et al.*, 2010). The region demonstrates moderate-to-high rates of diffuse seismicity in the vicinity of the fault (Power, 1988; Meighan *et al.*, 2013). Additionally, geological evidence based on seismic resuspension of lake sediments suggests that large paleoseismic events on the Duke River-Denali fault system may have occurred as recently as 300-500 years before present (Doig, 1998).

The Duke River fault is modelled as an approximately SSW dipping line source with a dip of 35°, based on the observations of Cobbett *et al.* (2010). The fault is assumed to propagate from the surface to a depth of 15 km, having a down-dip rupture width of approximately 26 km. The preferred slip rate of 3.5 mm/yr was determined as the vector sum of published dextral strike-slip motion and crustal shortening slip rates (Leonard *et al.*, 2008). The fault's MFD was subsequently calculated using the methods described in Section 3 using a M_{min} of 6.5 and M_{max} of 7.7. Two equally weighted MFDs are used in the hazard model: one assuming $b = 0.8$ and the other using a pseudo-characteristic MFD.

The Duke River fault lies within the Denali South Region (DCR) areal source zone. Despite the presence of two significant earthquake generators (the Duke River and Eastern Denali faults), the zone's M_{max} is retained at M_W 7.2 because of an apparent off-fault earthquake in 1901 with a magnitude of M_W 7.1 (Halchuk *et al.*, 2015). Given the location uncertainties for earthquakes of this vintage, it is possible that this earthquake did occur on one of the modelled faults, but this cannot be confirmed.

6. The Beaufort-Mackenzie Convergence

The Mackenzie Delta is the world's second largest Arctic delta and the Beaufort-Mackenzie Basin comprises up to 16 km-thick sediments overlying oceanic crust (Stephenson *et al.*, 1994). It is also well-recognised as a Cretaceous-to-Holocene thrust zone (Lane, 2002). Simple regional tectonic models, supported by GPS deformation rates (Leonard *et al.*, 2007), suggest that the northerly motion from the Yukon continues to the Beaufort Sea margin (Hyndman *et al.*, 2005a; Leonard *et al.*, 2007). These models assume convergence between right-lateral motion in the Richardson Mountains region to left-lateral motion in the Canning displacement zone in eastern Alaska as suggested by earthquake focal mechanisms (Biswas and Tytgat, 1988). However, this inferred crustal deformation appears inconsistent with contemporary seismicity within the Beaufort-Mackenzie region. Hyndman *et al.* (2005a) suggest that there may be thrusting of the delta sediment section and continental crust over the oceanic lithosphere, with the shallow-dipping detachment at the top of the oceanic crust. Consequently, there is the possibility

that inferred convergence based on GPS data and seismicity data south of the Mackenzie Delta region could manifest itself through infrequent large earthquakes with very few small events (Hyndman *et al.*, 2005a), similar to the Cascadia subduction zone. An alternative hypothesis is that the strain is being released through aseismic slip and does not induce earthquakes.

For the 2015 NBCC hazard models, the Beaufort-Mackenzie Convergence (BMC) areal source zone is defined about the inferred region of crustal deformation (see Fig. 1c). Based on our preferred slip rate of 2 mm/yr, M_{min} of 7.0 and M_{max} of 7.8, a pseudo-characteristic MFD is estimated using Equation 5. Since we can only speculate on the nature of this source based on GPS slip deficits, seismicity to the south and favourably oriented geological structure beneath the delta sediments, we allow for the possibility of both large rare earthquakes as well as aseismic slip (i.e., no earthquakes) with an equal weight.

7. Hazard Sensitivity

7.1. Areal Sources

The use of a multi-tiered GIS framework for source zone definition has allowed for the improved representation of geological and geophysical characteristics for the 2015SHMC in the western Arctic. The ability of overlaying multiple datasets enabled the authors to better define the seismotectonic domains in which future seismicity is likely to occur. As a consequence, significant adjustments in hazard have occurred in the Richardson Mountains region, where an improved earthquake catalogue Halchuk *et al.* (2015) and use of geological and geophysical information led to the confinement of seismicity within a smaller area than in the past. Furthermore, hazard in the Eskimo Lakes, Northwest Territories, region has also increased due to a reassessment of the source zones to align with geological features, again confining contemporary seismicity within smaller regions. Adjustments along the northern boundary of the southwestern Canadian model (Halchuk *et al.*, 2014; Rogers *et al.*, 2015) have also led to an increase in hazard at around 60° N by confining historical seismicity to the northern model.

7.2. Fault Sources

The introduction of new fault sources within the 2015SHMC has generally resulted in an increase in hazard in the regions immediately adjacent to these features. In particular, the addition of the HGT has led to an increase to the hazard on Haida Gwaii because it has made the fault source more proximal nearby settlements; in particular the Village of Queen Charlotte. Significant increases in hazard are also observed near the crustal faults in Yukon Territory: in particular, the Denali and Duke River faults.

7.3. Ground-Motion Model Selection

A large uncertainty in modelling earthquake hazard is the selection of ground-motion models (GMMs). In the western Arctic region, all areal sources use active crustal GMMs as proposed for western Canada by Atkinson and Adams (2013). Crustal and offshore strike-slip faults also use active western crustal GMMs. Offshore thrust faults use subduction interface GMMs as they are assumed to be an analogue for this tectonic environment. Subsequent to decisions for the proposed NBCC2015 hazard model, Allen and Brillon (2015) compared modern GMMs (including those proposed for the NBCC2015) against recorded ground motions from the 2012 Haida Gwaii earthquake sequence on the HGT. Ground motions from these events appear to yield lower shaking than either the interface or crustal GMPEs as proposed for the NBCC2015 by factors of 2 or more across much of the spectral range. Consequently, if future HGT events are similar to the 2012 mainshock and aftershocks, then the use of modern GMMs may overestimate the hazard near the offshore regions of western Canada. However, more testing and evaluation of GMMs for future use is required.

The sensitivity of the calculated hazard to the choice of GMM is shown for individual faults in the Haida Gwaii region (Fig. 5). Hazard contributions from the HGT using the Atkinson and Adams (2013) subduction interface GMMs are approximately twice those of the QCSS using crustal GMPEs. If hazard for HGT is calculated with crustal GMPEs instead of the interface GMPEs, the hazard is similar to the hazard from QCSS; therefore the different tectonic nature of the fault sources is very important for modelling ground shaking hazard.

8. Concluding Remarks

This contribution documents the development of the western Arctic seismic hazard model as proposed for the NBCC2015. The model, for the first time, includes crustal fault sources and adds additional offshore

faults. A number of the proposed changes increase the hazard at many localities. This is largely due to an improved understanding of the earthquake fault sources from paleoseismic studies and GPS observations, particularly following the recent 2012 Haida Gwaii earthquake sequence. The use of a multi-tiered GIS framework has also allowed for refinement of areal source zone boundaries to isolate contemporary seismicity to regions of similar geological and geophysical characteristics.

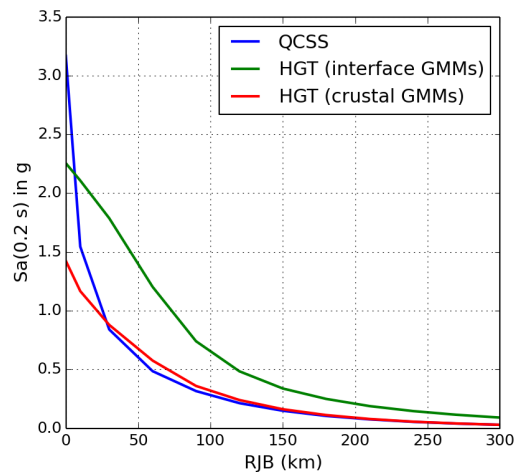


Figure 5 – Sensitivity test showing the individual contributions to seismic hazard along a profile approximately normal to the plate boundary from the QCSS and the HGT. The hazard for HGT is calculated using both subduction interface (as proposed for the 2015 NBCC hazard model) and active shallow crustal GMMs. The seismic hazard shown is the mean hazard for $S_a(0.2\text{ s})$ p.a. on a site at the Soil Class B/C boundary. Note the large decrease in hazard if HGT is modelled using crustal GMMs. The hazard model in these regions is thus dominated by the HGT using subduction interface GMMs.

9. Acknowledgements

The authors are thankful to many of our colleagues within the Geological Survey of Canada whose knowledge and expertise helped refine earthquake sources in the western Arctic and adjacent offshore regions. In particular, we thank Roy Hyndman, Lucinda Leonard and Earl Davis. Roy Hyndman and John Cassidy are thanked for their critical reviews of this manuscript. This is ESS contribution number 20150113. © Her Majesty the Queen in right of Canada 2015.

10. References

- ADAMS, J., and HALCHUK, S. (2003). Fourth generation seismic hazard maps of Canada: values for over 650 Canadian localities intended for the 2005 National Building Code of Canada, *Geological Survey of Canada Open File 4459*, 155 pp, doi:10.4095/214223.
- ADAMS, J., HALCHUK, S., ALLEN, T., and ROGERS, G. (2015). Canada's 5th Generation seismic hazard model for the 2015 National Building Code of Canada, *11th Canadian Conference on Earthquake Engineering*, 21–24 July, Victoria, Canada, Paper 93775.
- AKI, K. (1965). Maximum likelihood estimate of b in the formula $\log N = a - bM$ and its confidence limits, *Bull. Earthq. Res. Inst.*, Vol. 43, pp. 237-239.
- ALLEN, T.I., and BRILLON, C. (2015). Assessment of ground-motion attenuation in the British Columbia north coast region, *Bull. Seism. Soc. Am.*, Vol. 105, No. 2B, pp. 1193-1205
- ATKINSON, G.M., and ADAMS, J. (2013). Ground motion prediction equations for application to the 2015 Canadian national seismic hazard maps, *Can. J. Civ. Eng.*, Vol. 40, pp. 988–998, doi: 10.1139/cjce-2012-0544.
- BAKER, J.W. (2008). An introduction to Probabilistic Seismic Hazard Analysis (PSHA) *Version 1.3pp*.
- BANKEY, V., CUEVAS, A., DANIELS, D., FINN, C.A., HERNANDEZ, I., HILL, P., KUCKS, R., MILES, W., PILKINGTON, M., ROBERTS, C., ROEST, W., RYSTROM, V., SHEARER, S., SNYDER, S., SWEENEY, R., VELEZ, J., PHILLIPS, J.D., and RAVAT, D. (2002). Digital data grids for the magnetic anomaly map of North Americapp, <http://pubs.usgs.gov/of/2002/ofr-02-414/>.
- BASHAM, P.W., FORSYTH, D.A., and WETMILLER, R.J. (1977). The seismicity of northern Canada, *Can. J. Earth Sci.*, Vol. 14, pp. 1646-1667.
- BILEK, S.L., and LAY, T. (1999). Rigidity variations with depth along interplate megathrust faults in subduction zones, *Nature*, Vol. 400, No. 29 July 1999, pp. 443-446.

- BISWAS, N.N., and TYTGAT, G. (1988). Intraplate seismicity in Alaska, *Seism. Res. Lett.*, Vol. 59, No. 4, pp. 227-233.
- BRAUNMILLER, J., and NÁBĚLEK, J. (2002). Seismotectonics of the Explorer region, *J. Geophys. Res.*, Vol. 107, No. B10, pp. 2208, doi:10.1029/2001JB000220.
- BROWN, A., and GIBSON, G. (2004). A multi-tiered earthquake hazard model for Australia, *Tectonophys.*, Vol. 390, pp. 25-43, doi: 10.1016/j.tecto.2004.03.019.
- BRUNE, J.N. (1970). Tectonic stress and the spectra of seismic shear waves from earthquakes, *J. Geophys. Res.*, Vol. 75, No. 26, pp. 4997-5009.
- CASSIDY, J.F., ELLIS, R.M., KARAVAS, C., and ROGERS, G.C. (1998). The northern limit of the subducted Juan de Fuca plate system, *J. Geophys. Res.*, Vol. 103, No. B11, pp. 26,949-26,961.
- CLAGUE, J.J. (1979). The Denali fault system in southwest Yukon Territory - A geologic hazard? *Current Research Part A, Geological Survey of Canada Paper 79-1A*, 50-56 pp.
- CLARK, D., MCPHERSON, A., and VAN DISSEN, R. (2012). Long-term behaviour of Australian stable continental region (SCR) faults, *Tectonophys.*, Vol. 566-567, pp. 1-30.
- COBBETT, R., ISRAEL, S., and MORTENSEN, J. (2010). The Duke River Fault, southwest Yukon: Preliminary examination of the relationships between Wrangellia and the Alexander terrane, *Yukon Exploration and Geology 2009*. L. H. Weston, and L. R. Blackburn, Yukon Geological Survey 143-158.
- DAVIS, E.E., and HYNDMAN, R.D. (1989). Accretion and recent deformation of sediments along the northern Cascadia subduction zone, *Geol. Soc. Am. Bull.*, Vol. 101, pp. 1465-1480.
- DAVIS, E.E., and RIDDIHOUGH, R.P. (1982). The Winona Basin: structure and tectonics, *Can. J. Earth Sci.*, Vol. 19, pp. 767-788.
- DEMETS, C., and DIXON, T.H. (1999). New kinematic models for Pacific-North America motion from 3 Ma to present, I: Evidence for steady motion and biases in the NUVEL-1A model, *Geophys. Res. Lett.*, Vol. 26, No. 13, pp. 1921-1924.
- DOIG, R. (1998). Paleoseismological evidence from lake sediments for recent movement on the Denali and other faults, Yukon Territory, Canada, *Tectonophys.*, Vol. 296, pp. 363-370.
- FLETCHER, H.J., and FREYMUELLER, J.T. (2003). New constraints on the motion of the Fairweather fault, Alaska, from GPS observations, *Geophys. Res. Lett.*, Vol. 30, No. 3, pp. 1139.
- GEM FOUNDATION. (2012). *Magnitude-frequency distributions*, Retrieved 31 December 2013, from <http://docs.openquake.org/oq-hazardlib/mfd.html>.
- GENERAL BATHYMETRIC CHART OF THE OCEANS (2008). The GEBCO_08 Grid, *International Hydrographic Organization and the Intergovernmental Oceanographic Commission of UNESCO*, 19 pp, <http://www.gebco.net/>.
- GUTENBERG, B., and RICHTER, C.F. (1944). Frequency of earthquakes in California, *Bull. Seism. Soc. Am.*, Vol. 34, No. 4, pp. 185-188.
- HAEUSSLER, P.J., SCHWARTZ, D.P., DAWSON, T.E., STENNER, H.D., LIENKAEMPER, J.J., SHERROD, B., CINTI, F.R., MONTONE, P., CRAW, P.A., CRONE, A.J., and PERSONIUS, S.F. (2004). Surface rupture and slip distribution of the Denali and Totschunda faults in the 3 November 2002 **M** 7.9 earthquake, Alaska, *Bull. Seism. Soc. Am.*, Vol. 94, No. 6B, pp. S23-S52.
- HALCHUK, S., ALLEN, T.I., ADAMS, J., and ROGERS, G.C. (2014). Fifth generation seismic hazard model input files as proposed to produce values for the 2015 National Building Code of Canada, *Geological Survey of Canada Open File 7576*, 15 pp, doi:10.4095/293907.
- HALCHUK, S., ALLEN, T.I., ROGERS, G.C., and ADAMS, J. (2015). Seismic Hazard Earthquake Epicentre File (SHEEF2010) used in the Fifth Generation Seismic Hazard Maps of Canada, *Geological Survey of Canada Open File XXXX*pp.

- HANKS, T.C., and BAKUN, W.H. (2002). A bilinear source-scaling model for M-log A observations of continental earthquakes, *Bull. Seism. Soc. Am.*, Vol. 92, No. 5, pp. 1841-1846.
- HANKS, T.C., and KANAMORI, H. (1979). A moment magnitude scale, *J. Geophys. Res.*, Vol. 84, No. B5, pp. 2348–2350.
- HYNDMAN, R.D. (2015). Tectonics and structure of the Queen Charlotte Fault Zone, Haida Gwaii: and large thrust earthquakes, *Bull. Seism. Soc. Am.*, Vol. 105, No. 2B, pp. 1058-1075.
- HYNDMAN, R.D., CASSIDY, J.F., ADAMS, J., ROGERS, G.C., and MAZZOTTI, S. (2005a). Earthquakes and seismic hazard in the Yukon-Beaufort Mackenzie, *CSEG Recorder*, Vol. May 2005, pp. 32–67.
- HYNDMAN, R.D., FLÜCK, P., MAZZOTTI, S., LEWIS, T.J., RISTAU, J., and LEONARD, L. (2005b). Current tectonics of the northern Canadian Cordillera, *Can. J. Earth Sci.*, Vol. 42, pp. 1117–1136.
- HYNDMAN, R.D., and HAMILTON, T.S. (1993). Queen Charlotte area Cenozoic tectonics and volcanism and their association with relative plate motions along the northeastern Pacific margin, *J. Geophys. Res.*, Vol. 98, No. B8, pp. 14,257-14,277.
- HYNDMAN, R.D., and WEICHERT, D.H. (1983). Seismicity and rates of relative motion on the plate boundaries of Western North America, *Geophys. J. R. astr. Soc.*, Vol. 72, pp. 59-82.
- JAMES, T., ROGERS, G., CASSIDY, J., DRAGERT, H., HYNDMAN, R., LEONARD, L., NYKOLAISHEN, L., RIEDEL, M., SCHMIDT, M., and WANG, K. (2013). Field studies target 2012 Haida Gwaii earthquake, *Eos*, Vol. 94, No. 22, pp. 197–198, doi: 10.1002/2013EO220002.
- KALBAS, J.L., FREED, A.M., and RIDGWAY, K.D. (2008). Contemporary fault mechanics in southern Alaska, *Active tectonics and seismic potential of Alaska*, American Geophysical Union. Geophysical Monograph Series 179, 321-336, doi: 10.1029/179GM18.
- LAMONTAGNE, M., HALCHUK, S., CASSIDY, J.F., and ROGERS, G.C. (2008). Significant Canadian earthquakes of the period 1600–2006, *Seism. Res. Lett.*, Vol. 79, No. 2, pp. 211-223.
- LANE, L.S. (2002). Tectonic evolution of the Canadian Beaufort Sea - Mackenzie Delta region: A brief review, *CSEG Recorder*, Vol. February, 2002, pp. 49-56.
- LAY, T., LE, L., KANAMORI, H., YAMAZAKI, Y., CHEUNG, K.F., KWONG, K., and KOPER, K.D. (2013). The October 28, 2012 Mw 7.8 Haida Gwaii underthrusting earthquake and tsunami: Slip partitioning along the Queen Charlotte Fault transpressional plate boundary, *Earth Planet. Sci. Lett.*, Vol. 375, pp. 57–70, doi: 10.1016/j.epsl.2013.05.005.
- LEONARD, L.J., HYNDMAN, R.D., MAZZOTTI, S., NYKOLAISHEN, L., SCHMIDT, M., and HIPPCHEN, S. (2007). Current deformation in the northern Canadian Cordillera inferred from GPS measurements, *J. Geophys. Res.*, Vol. 112, No. B11401, pp. doi:10.1029/2007JB005061.
- LEONARD, L.J., MAZZOTTI, S., and HYNDMAN, R.D. (2008). Deformation rates estimated from earthquakes in the northern Cordillera of Canada and eastern Alaska, *J. Geophys. Res.*, Vol. 113, No. B08406, pp. doi:10.1029/2007JB005456.
- LEONARD, L.J., ROGERS, G.C., and MAZZOTTI, S. (2012). A preliminary tsunami hazard assessment of the Canadian coastline, 126 pp, doi: 10.4095/292067.
- LEONARD, M. (2010). Earthquake fault scaling: self-consistent relating of rupture length, width, average displacement, and moment release, *Bull. Seism. Soc. Am.*, Vol. 100, No. 5A, pp. 1971–1988.
- LIU, M., and WANG, H. (2012). Roaming earthquakes in China highlight midcontinental hazards, *EOS*, Vol. 93, No. 45, pp. 453-454.
- MATMON, A., SCHWARTZ, D.P., HAEUSSLER, P.J., FINKEL, R., LIENKAEMPER, J.J., STENNER, H.D., and DAWSON, T.E. (2006). Denali fault slip rates and Holocene–late Pleistocene kinematics of central Alaska, *Geol.*, Vol. 34, No. 8, pp. 645–648, doi: 10.1130/G22361.1.

- MAZZOTTI, S., HYNDMAN, R.D., FLÜCK, P., SMITH, A.J., and SCHMIDT, M. (2003). Distribution of the Pacific/North America motion in the Queen Charlotte Islands-S. Alaska plate boundary zone, *Geophys. Res. Lett.*, Vol. 30, No. 14, pp. 1762, doi:10.1029/2003GL017586.
- MEIGHAN, L., CASSIDY, J.F., MAZZOTTI, S., and PAVLIS, G.L. (2013). Microseismicity and tectonics of southwest Yukon Territory, Canada using a local dense seismic array, *Bull. Seism. Soc. Am.*, Vol. 103, No. 6, pp. 3341-3346, doi: 10.1785/0120130068.
- MILES, W.F., ROEST, W.R., and VO, M.P. (2000a). Gravity Anomaly Map, Canada, Geological Survey of Canada, Open File 3830a.
- MILES, W.F., ROEST, W.R., and VO, M.P. (2000b). Magnetic Anomaly Map, Canada, Geological Survey of Canada, Open File 3829a.
- NISHENKO, S.P., and JACOB, K.H. (1990). Seismic potential of the Queen Charlotte-Alaska-Aleutian seismic zone, *J. Geophys. Res.*, Vol. 95, No. B3, pp. 2511-2532.
- POWER, M.A. (1988). Mass movement, seismicity and neotectonics in the northern St. Elias Mountains, Yukon, Department of Physics. Edmonton, AB, University of Alberta. Vol. MSc, pp. 125.
- ROGERS, G., ADAMS, J., HALCHUK, S., and ALLEN, T. (2015). NBCC2015 seismic hazard for southwest British Columbia, *11th Canadian Conference on Earthquake Engineering*, 21–24 July, Victoria, Canada
- SALTUS, R.W., BROWN II, P.J., MORIN, R.L., and HILL, P.L. (2008). 2006 compilation of Alaska gravity data and historical reportspp, <http://pubs.usgs.gov/ds/264/>.
- SHAW, B.E. (2009). Constant stress drop from small to great earthquakes in magnitude-area scaling, *Bull. Seism. Soc. Am.*, Vol. 99, No. 2A, pp. 871–875, doi: 10.1785/0120080006.
- STEPHENSON, R.A., COFLIN, K.C., LANE, L.S., and DIETRICH, J.R. (1994). Crustal structure and tectonics of the southeastern Beaufort Sea continental margin, *Tectonics*, Vol. 13, No. 2, pp. 389-400,.
- STOCKWELL, C.H. (1968). Tectonic map of Canada, *Geol. Surv. Canada, 1251 A 1251 App*.
- STRASSER, F.O., ARANGO, M.C., and BOMMER, J.J. (2010). Scaling of the source dimensions of interface and intraslab subduction-zone earthquakes with moment magnitude, *Seism. Res. Lett.*, Vol. 81, No. 6, pp. 941-950, doi: 10.1785/gssrl.81.6.941.
- WANG, K., HE, J., SCHULZECK, F., HYNDMAN, R.D., and RIEDEL, M. (2015). Thermal condition of the 27 October 2012 M_w 7.8 Haida Gwaii subduction earthquake at the obliquely convergent Queen Charlotte margin, *Bull. Seism. Soc. Am.*, Vol. 105, No. 2B, doi: 10.1785/0120140183.
- WEICHERT, D.H. (1980). Estimation of the earthquake recurrence parameters for unequal observation periods for different magnitudes, *Bull. Seism. Soc. Am.*, Vol. 80, No. 70, pp. 1337-1346.
- WELLS, D.L., and COPPERSMITH, K.J. (1994). New empirical relationships among magnitude, rupture length, rupture width, rupture area, and surface displacement, *Bull. Seism. Soc. Am.*, Vol. 84, No. 4, pp. 974-1002.
- WESSON, R.L., BOYD, O.S., MUELLER, C.S., BUFE, C.G., FRANKEL, A.D., and PETERSEN, M.D. (2007). Revision of time-independent probabilistic seismic hazard maps for Alaska, *U.S. Geological Survey Open-File Report 2007-1043*, 33 pp.
- YOUNGS, R.R., and COPPERSMITH, K.J. (1985). Implications of fault slip rates and earthquake recurrence models to probabilistic seismic hazard estimates, *Bull. Seism. Soc. Am.*, Vol. 75, No. 4, pp. 939-964.
- YUAN, T., SPENCE, G.D., and HYNDMAN, R.D. (1992). Structure beneath Queen Charlotte Sound from seismic-refraction and gravity interpretations, *Can. J. Earth Sci.*, Vol. 29, pp. 1509- 1529.